applied sciences

MDPI

Article

Optimization Design of Filament Wound Composite Pressure Vessel Based on OpenSees

Binbin Dai, Mingjue Zhou *, Jianye Zhang, Yuebing Li and Weiya Jin

Institute of Process Equipment and Control Engineering, College of Mechanical Engineering, Zhejiang University of Technology, Hangzhou 310023, China; 13758145694@163.com (B.D.); 15058885844@163.com (J.Z.)
* Correspondence: zhoumingjue@163.com

Abstract: Composite pressure vessels have the characteristics of light weight, corrosion resistance, good sealing, and high reliability, and have been widely used in military and civilian applications. With the widespread use of composite pressure vessels today, determining how to conduct scientific research and correct analysis becomes very important. With the continuous development of computer technology and the continuous improvement of finite element algorithms, the numerical calculation method has become an important method for studying composite pressure vessels. In this paper, the finite element analysis of filament wound composite pressure vessels is carried out by means of ANSYS and OpenSees. The semi-analytical method is used to optimize the design with the help of the Python tool. The parametric language is used to design different fiber layer schemes. The optimal fiber layer scheme is obtained by Nelder-Mead optimization function optimization. The optimal angle and thickness obtained after multiple iterations are 9.96875° and 0.03325 m, respectively.

Keywords: composite pressure vessel; fiber ply; optimization design

check for updates

Citation: Dai, B.; Zhou, M.; Zhang, J.; Li, Y.; Jin, W. Optimization Design of Filament Wound Composite Pressure Vessel Based on OpenSees. *Appl. Sci.* **2023**, *13*, 4894. https://doi.org/10.3390/app13084894

Academic Editor: Antonio Miotello

Received: 20 March 2023
Revised: 6 April 2023
Accepted: 11 April 2023
Published: 13 April 2023

Copyright: © 2023 by the authors. Licensee MDPI, Basel, Switzerland. This article is an open access article distributed under the terms and conditions of the Creative Commons Attribution (CC BY) license (https://creativecommons.org/licenses/by/4.0/).

1. Introduction

Carbon fiber composite material refers to a new type of composite material with high specific strength, high specific stiffness, high-temperature resistance, and good designability, which is formed by using carbon fiber or carbon fiber fabric as reinforcement, resin as a matrix, and certain composite methods [1]. Due to the good mechanical properties and chemical stability of carbon fiber composites, it undertakes the important task of new product development and technological breakthrough in major national strategic fields such as energy, transportation, aerospace, national defense, and military industry. Especially in the field of national defense and military industry, special materials represented by carbon fiber composite materials play an irreplaceable role in the upgrading of weapons and equipment and the research of new models [2].

The structural analysis and optimization design of composite pressure vessels have very important theoretical significance and engineering application value. Fiber winding is a technology for manufacturing composite structures. This technology uses a stationary rotating mandrel, and the guide arm moves horizontally with the mandrel [3]. There is a curved eye on the arm, which is used to group and distribute pre-impregnated fibers, called roving. When the mandrel rotates, the roving is wound on the surface of the mandrel to form a composite winding. The accurate direction of the composite winding is determined by the conveying rate and the rotation speed of the mandrel. The fiber is impregnated in the resin before wrapping the mandrel and then cured with the fiber. After the fiber coating is completed, the entire component, mandrel and composite coating are placed into the oven and heated and cured at the required temperature. When the composite resin [4] is completely cured, the mandrel is removed, leaving the hollow composite structure. The winding angle, fiber thickness, and layering method of the fiber winding layer have a great influence on the overall performance of the composite pressure vessel. Determining how

to determine the optimal value of these parameters is a major problem in the design and production of composite pressure vessels [5].

With the continuous advancement of computer and software technology, fine modeling has gradually become an effective method. At present, SAP2000, ANSYS, ABAQUS, OpenSees, etc. have been widely used in the world, and a large number of numerical simulations and parametric studies have been carried out on composite pressure vessels. By comparing the effects of different winding angles on the stress of carbon fiber composite pressure vessels, Arhant et al. [6] determined the failure according to the maximum strain criterion, the maximum stress criterion, and the Tsai-Wu failure criterion. It was found that the performance of the pressure vessel when the fiber winding angle was 51° was significantly better than that of other pressure vessels. Li Changpeng et al. [7] used the grid theory and finite element model to design the carbon fiber winding ultra-high pressure pre-mixed abrasive tank, which reduced the mass of the traditional abrasive tank by 80%, and the mechanical performance of the tank was better. Chen Xiaoping [8] aimed at the current situation in which the research and application of high-strength medium modulus T800 carbon fiber are less, and the T800 carbon fiber fully wound composite pressure vessels with different diameters were obtained by the dry winding process, which laid a theoretical and experimental foundation for the industrial application of high performance T800 carbon fiber.

In the existing literature, the FEA methods used in the design of filament wound pressure vessels mainly include special analysis and standard analysis.

(a) Special analysis methods mainly include special one-dimensional, two-dimensional, and three-dimensional finite elements, the Ritz method, finite differences, and other linear and nonlinear analyses. These are advanced analysis methods with high analysis accuracy and computational efficiency.

(b) Standard analysis methods Some standard industrial programs such as NASTRAN, ANSYS, ABAQUS, and GENESIS also can analyze the mechanical properties of filament wound pressure structures. These standard programs are based on the displacement of the finite element method with powerful functions, good numerical properties, simplicity, universality, and versatility [9].

Optimal design is a new design idea proposed in the 1960s. It applies the optimization principle and computer technology to the design and proposes an important method for scientific design in engineering. Firstly, under the given design constraints, the design problem in the project is transformed into an optimal problem, and then the computer is used as a tool to find the optimal design scheme to achieve the predetermined design goal. This has greatly improved the efficiency and quality of design, which is widely used in various product designs and various industrial design fields.

In the field of intelligent optimization computing, there are two swarm intelligence algorithms: ant colony optimization algorithm and particle swarm optimization algorithm. The former is derived from the simulation of the food-searching behavior of the ant community and has been successfully applied to many combinatorial optimization problems. These small particles, called “swarms”, can adjust their trajectory and fly to the best position they have experienced before as well as the best position other particles have experienced. All particles should adjust their speed and remember the best position they have experienced to achieve this goal. By coordinating and communicating with each other, particles always follow the optimal particles in the solution space to search, so they have faster computational efficiency [10–13].

Based on the above background, this paper uses the combination of OpenSees and ANSYS to carry out finite element analysis of composite pressure vessels and uses the optimization method of Nelder-Mead to optimize the fiber angle and fiber thickness in the filament winding part. This method can simplify the calculation process and find the best winding scheme through function optimization, which has certain guiding significance for the fiber winding layer of a composite winding structure.

2. Finite Element Analysis

The development of composite pressure vessel design is still quite primitive. Usually, only limited analysis is performed to obtain the initial design, and then the design is improved by several "build and explode" iterations. However, the material and resource costs of manufacturing multiple test pieces are extremely high. To reduce costs, finite element analysis (FEA) is often used to reduce the number of iterations required. If performed manually, this process may be very cumbersome and time-consuming. Therefore, the finite element analysis process is used to avoid multiple iterations [14].

The standard process of finite element analysis includes defining the model and its load and solving and interpreting the results. If the solution results show that it is necessary to modify the design, then the geometric structure or load of the model must be changed and the above steps must be repeated. Especially when the model is more complex or modified, this process may be expensive and time-consuming. APDL provides users with the function of automatically completing the above cycle using establishing intelligent analysis. In other words, the input of the program can be set to be determined according to the specified functions, variables, and selected analysis criteria [15]. It allows complex data input, giving users control over any design or analysis property, such as geometry, material, boundary conditions, and mesh density, extending capabilities beyond traditional finite element analysis, and extending more advanced operations, including sensitivity studies, parametric modeling of parts, design modifications, and design optimization [16].

Parametric modeling is an important technical means to solve engineering problems by using numerical calculation software. The special structural characteristics of wound pressure vessels complicate the process of parametric modeling [17]. Chen Dan [18] determined the winding tension value through the lining stability analysis, and gave the design of the winding layer by the grid theory. Combined with the linear design and simulation, the winding process of two yarns, five tangent points, and geodesics was determined. Based on this parameter, the accurate modeling of the winding pressure vessel was realized, and the strength analysis of the structure was completed by the finite element software ABAQUS. Using the designed winding parameters, through the four-axis CNC filament winding machine, using T800 carbon fiber and EW-6F epoxy resin, the winding process of two-strand yarn, five-tangent point, and geodesic line was used to complete the molding of a plastic liner carbon fiber fully wound type IV composite pressure vessel. During the winding process, the fibers are evenly and stably distributed on the surface of the inner liner. The number of complete cycles required for the spiral layer to be wrapped is consistent with the line shape simulation results, which confirms the accuracy of the design parameters. Zeng Wenlei [19] determined the angle of the fiber winding layer of the pressure vessel according to the winding forming theory. The spiral winding angle is 19.38°, the circumferential winding angle is 89.14°, the thickness of the winding layer is 0.375 mm, the winding layer is three layers, and the fiber layer is six layers. By establishing the finite element model of the container on the basis of CADWIND, the line type, number of layers, angle, and thickness of the winding layer are designed and analyzed as the finite element model data, and compared with the subsequent experiments. In the hydraulic blasting experiment, after 8 h of curing, the finished product is glued and unglued at the head. The two groups of comparative experiments show that the sealing performance of the glue group is good, which is consistent with the finite element simulation results, and the error is 1.2%. The experimental process and the specific blasting experimental data show that the results of CADWIND and finite element simulation analysis are correct, and the parameters of analysis and design are feasible. From the above research status, it can be seen that the model data obtained by the finite element software to simulate the filament wound composite pressure vessel can be mutually verified with the experimental results, and the error is small. Therefore, it is feasible to simulate the filament wound composite pressure vessel by APDL in this paper.

2.1. APDL Analysis and Calculation

Two kinds of elements can be used for finite element analysis of composite models, namely laminated elements and anisotropic elements. In ANSYS, the laminated elements of composite materials include shell91, shell99, and shell181 elements [20]. The introduction of different unit types is shown in Table 1. The elements typically used in this paper are shell181 elements.

Table 1. Shell element categories and introduction [21].

Element Types	Introduction
Shell99	Linear shell element for thin or medium thickness elements with a thickness ratio of less than 1/10
Shell91	Nonlinear shell element, supporting large strain and plastic deformation.
Shell181	The finite element shell element supports the nonlinear behavior of most materials.
Solid46	Three-dimensional solid element for a solid structure.
Solid191	Three-dimensional solid element, high accuracy, does not support material nonlinearity and large deformation.

The research object of this paper is a certain type of filament wound composite pressure vessel, and the geometric parameters are shown in Table 2.

Table 2. Geometric parameters of composite pressure vessel (unit mm).

Diameter	Cylinder Length	Major Semiaxis	Minor Semiaxis
228	700	104	52

The mechanical properties of the material are elastic modulus 2×10^{11} MPa, Poisson's ratio 0.3, and density 2.7×10^{-9}.

The geometric model is established in the pre-processing of ANSYS, and the mesh is divided after defining the material properties and real constants. The order of fiber layer is shown in Figure 1. For the special and complex structure of the filament wound pressure vessel, to ensure the rules of the unit, the hexahedral mesh is used to divide the grid. A total of 2086 elements are divided. The mesh division of the finite element model is shown in Figure 2, and the fiber layer mesh is shown in Figure 3.

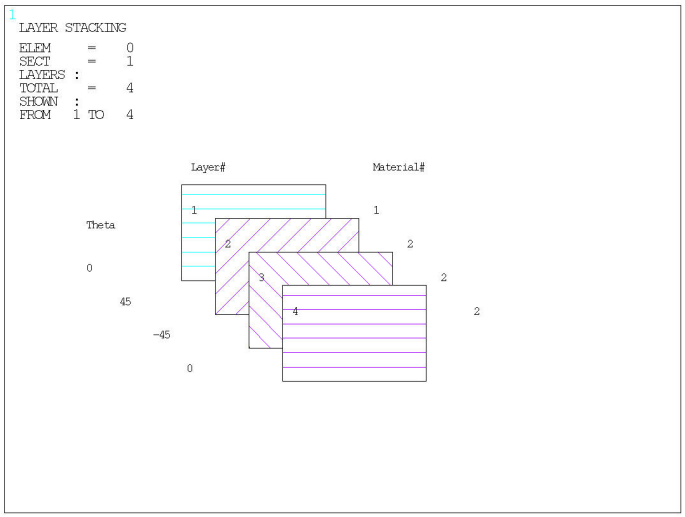


Figure 1. Diagram of fiber ply sequence and angle.

Referring to the actual situation, full constraints are applied to the bottom of the finite element model, and 30 MPa uniform internal pressure is applied on the inner wall. The stress and displacement contours output by APDL are shown in Figures 4 and 5.

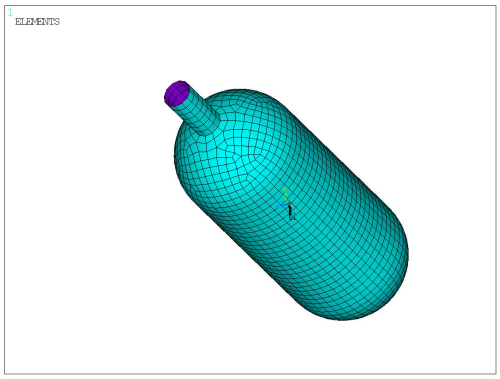


Figure 2. Model grid diagram.

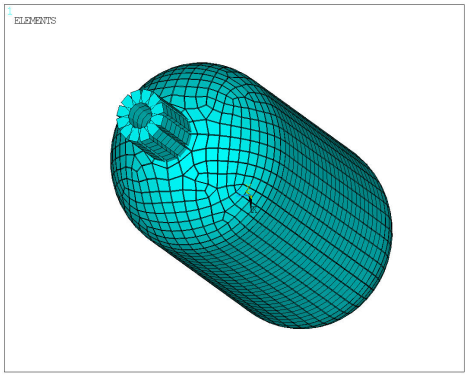


Figure 3. Fiber layer grid diagram.

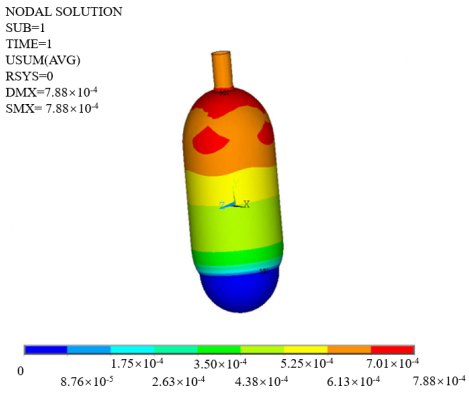


Figure 4. Displacement cloud diagram.

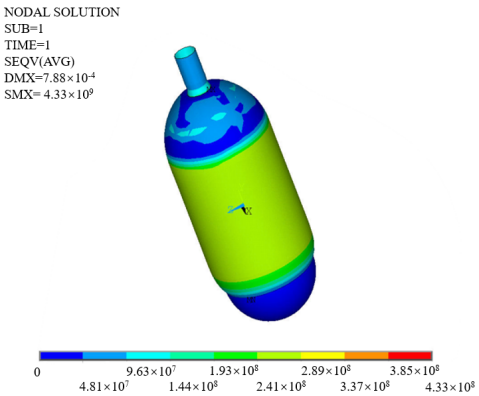


Figure 5. Stress cloud diagram.

2.2. OpenSees Program Analysis and Calculation

As an influential analysis program and development platform abroad, OpenSees also has the following outstanding features: easy to improve, easy to develop collaboratively and maintains international synchronization. OpenSees is mainly used for seismic response simulation of structure and rock [22]. The analysis that can be realized includes simple static linear elastic analysis, static nonlinear analysis, section analysis, modal analysis, pushover pseudodynamic analysis, dynamic linear elastic analysis, and complex dynamic nonlinear analysis; it can also be used to analyze the reliability and sensitivity of structures and geotechnical systems under earthquake action. Since its launch in 1999, the software has been continuously upgraded and improved, adding many new materials and units, introducing many mature Fortran library files for its use (such as FEAP, and FEDEAS materials), updating efficient and practical algorithms and convergence criteria, allowing multi-point input seismic wave records, and continuously improving the memory management level and computational efficiency in the operation, allowing users to control the analysis at the script level.

Based on the existing MITC4 shell element in OpenSees, Lu et al. [23] developed the layered shell section and the corresponding two-dimensional concrete constitutive and uniaxial reinforcement constitutive, and verified the reliability and versatility of the calculation model through a large number of shear wall tests. On this basis, Lu Xinzheng et al. used OpenSees software to establish a set of models suitable for high-rise and super high-rise structures, that is, the beam-column adopts the fiber cross-section model, and the shear wall and core tube adopt the layered shell model. The nonlinear elastic-plastic numerical simulation of several super high-rise buildings was carried out, and the conclusion was consistent with the numerical simulation results provided by the commercial software MSC.Marc, which confirmed the feasibility and reliability of the layered shell model applied to the seismic response study of super high-rise structures. This has certain guiding significance for simulating finite element model calculation with OpenSees.

OpenSees modeling calculation can be divided into the initial setting, node space position, constraint definition, interface attribute definition, shell element definition and composition, load definition, record output definition, static analysis definition, and calculation time definition.

When creating a finite element model, it is necessary to first determine the parameter values of the selected materials. The material parameters to be determined by the ShellMITC4 shell element model include the parameters of isotropic elastic material (nDMaterial ElasticIsotropic), uniaxial elastic material (uniaxialMaterial Elastic), material specification in the layered shell (nDMaterial PlateRebar), and section definition of the layered shell (section LayeredShell). The properties of uniaxial fiber materials are shown in Table 3.

Table 3. Properties of uniaxial fiber material.

Parameter/GPa	E_1	E_2	E_3	Nu_{12}	Nu_{13}	Nu_{23}	G_{12}	G_{13}	G_{23}
Numerical Value	145	8.2	8.2	0	0	0	4.5	4.5	3.5

The composite material has a total of three fiber layers in the barrel section, and different fiber winding angles and fiber thicknesses are set respectively. The ply scheme is shown in Tables 4 and 5.

Table 4. Fiber layer ply angle design scheme.

Scheme 1	Scheme 2	Scheme 3	Scheme 4	Scheme 5	Scheme 6	Scheme 7	Scheme 8
15	20	25	30	35	40	45	0
−15	−20	−25	−30	−35	−40	−45	0
0	0	0	0	0	0	0	0

Table 5. Fiber layer thickness design scheme.

Scheme 1	Scheme 2	Scheme 3	Scheme 4	Scheme 5	Scheme 6	Scheme 7	Scheme 8
0.001/m	0.002/m	0.003/m	0.004/m	0.005/m	0.006/m	0.007/m	0.008/m
0.001/m	0.002/m	0.003/m	0.004/m	0.005/m	0.006/m	0.007/m	0.008/m
0.001/m	0.002/m	0.003/m	0.004/m	0.005/m	0.006/m	0.007/m	0.008/m

The shell element used in this paper is the ShellMITC4 element, so the material command needs to be modified. The uniaxial elastic material is modified to a three-dimensional elastic material suitable for shell element analysis, that is, the elastic material considering Poisson's ratio. The ShellMITC4 element improves the bending performance of the thin plate by using a bilinear isoparametric representation combined with modified shear field interpolation. The so-called shell element has in-plane stiffness (membrane element, plane stress element), and also has in-plane stiffness (plate element). ShellMITC4 element is a four-node rectangular isoparametric element, as shown in Figure 6, the layered shell section model is shown in Figure 7, and the same shape function is used to describe the element displacement and element coordinates [24]. Although the element has a small number of nodes and a simple displacement mode, the discrete Mindlin technique is used to interpolate the transverse shear strain independently, so it can effectively eliminate the problems of shear locking and pseudo zero energy mode.

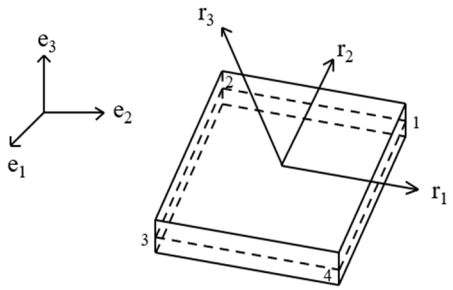


Figure 6. Four-node shell element.

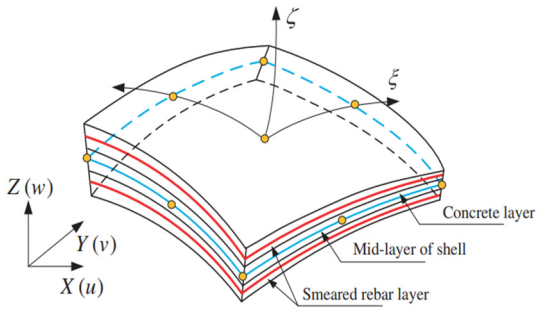


Figure 7. Shell element with a layered shell section model.

It is impossible to output stress-related data during output calculation. According to the literature, at present, the output mechanism of macroscopic force, displacement, and other information of elements or components (structures) in OpenSees is relatively mature, but the output mechanism of microscopic stress is still not perfect. From the code of OpenSees, it can be seen that the numerical model has no element stress output interface at the cross-section level, and no element stress output interface is found by viewing other groups of code. Therefore, the numerical model can only output the internal force and displacement of the element, but it cannot output specific stress information. Therefore, the form of directly recording stress information is adopted, and the corresponding order between the output data and the unit cannot be clearly defined in this form. In order to solve this problem, the output data need to be screened, and the screening process is shown in Figure 8.

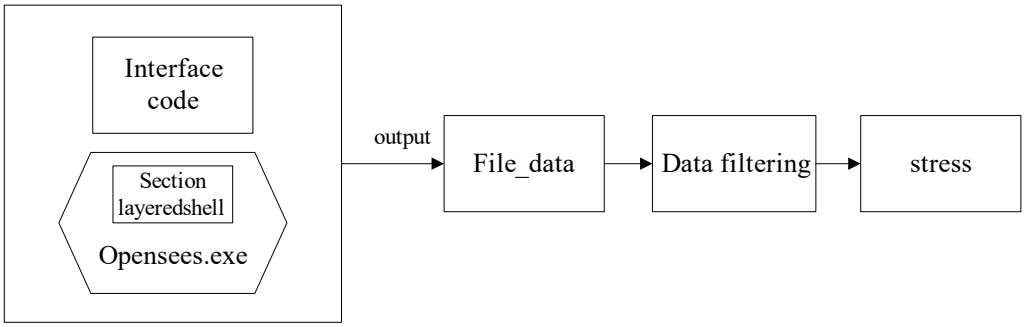


Figure 8. Stress extraction process.

(1) The interface program is written in C + + language to output stress. According to the characteristics of OpenSees software and the layered shell model's programming structure, the stress information's position is determined. Then the interface program is added to the programming structure of OpenSees, and OpenSees is recompiled to obtain a new OpenSees execution program [25].

(2) The composite pressure vessel is simulated to verify the program of the stress output interface. In this paper, the recompiled OpenSees program is used to simulate the existing tests, and the stress data of the composite pressure vessel are output and filtered. Firstly, according to the characteristics of the output data, the position of each displacement convergence step is determined in time. At the same time, the stress value of each element is determined by the order of elements in space and the order of output data.

The data filtering work includes two aspects: on the one hand, according to the characteristics of the output data, the position of the convergence step of each displacement step is determined in time; on the other hand, the corresponding relationship between the order of the unit and the order of the output data is determined in space, and the stress value of each unit is determined.

Combined with the above-mentioned design of the ply scheme, if APDL is used for calculation and analysis, only one data result of the scheme can be obtained at a time. For different scheme designs, it is necessary to repeatedly model and modify the parameters, and the output data file needs to be saved as many times as possible, otherwise, it cannot be retained for subsequent verification. That is, it uses the OpenSees parametric language to calculate, but also needs to write multiple running files, and undergo multiple runs to obtain the required data files. Based on these problems, a set of programs that can automatically analyze and process data is written. When writing the TCL file, for the same model, its node coordinates, unit information, constraint settings, load values, etc., are unchanged. What needs to be changed is only the material setting part and some parameters of the file output part. Therefore, only the material parameters of a specific row need to be modified, then multiple tcl files are output cyclically, and then the bat file (input OpenSees running environment variables, and the path of various library files) is written. It eliminates the process of compiling in the vs environment, and finally modifies the last line in the bat file so that multiple cmd windows can be opened simultaneously for parallel computing, greatly save computing time and improving efficiency.

After the completion of the calculation, the data are processed, and the output data file is extracted by Python, MATLAB, and other tools. The simulation results of composite pressure vessels with different ply modes are compared by different methods: the comparison of APDL simulation and OpenSees simulation results, as shown in Figure 9; the comparison of node displacement diagrams obtained from different angles of ply under OpenSees is shown in Figure 10; the comparison of node displacement diagrams obtained by different thickness layers are shown in Figure 11.

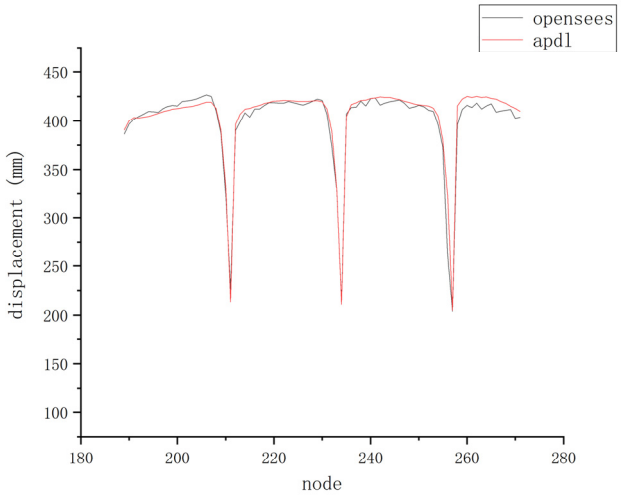


Figure 9. Comparison diagram of node displacement.

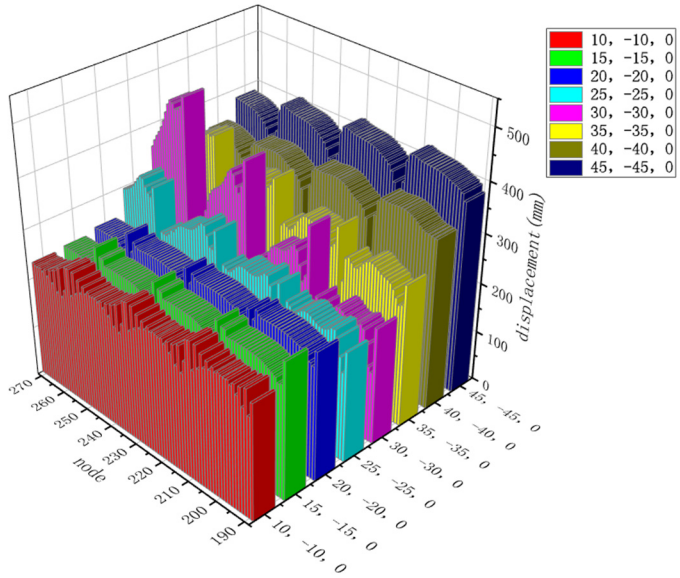


Figure 10. Node displacement diagrams at different angles.

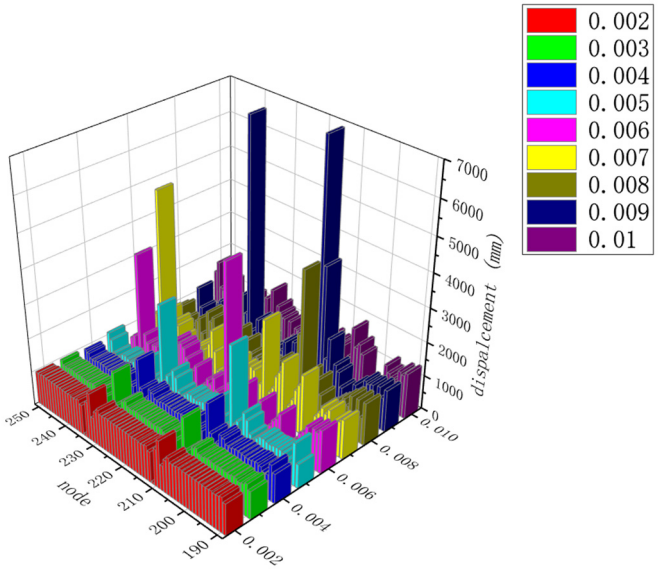


Figure 11. Node displacement diagrams under different thicknesses.

It can be seen from Figure 9 that the trend of node displacement simulated by different methods under the control variables is the same, and the numerical values are close. Therefore, the results of OpenSees simulating shellMITC4 can be trusted.

It can be seen from Figure 10 that the changing trend of node displacement is not large. With the increase of different ply angles, the node displacement also increases, and the range of fluctuation also gradually increases. In this figure, the scheme with a ply angle of 20°, −20°, and 0° has the most stable displacement and small fluctuation range.

It can be seen from Figure 11 that the displacement of the nodes in the previous schemes does not change much, and the fluctuation range is small. However, when the thickness gradually increases, the displacement of the nodes changes greatly, and the displacement of individual nodes increases sharply.

The stress that can be outputted by OpenSees is plane stress, while the output in APDL is the first, second, and third principal stresses. Therefore, it is necessary to solve the principal stress and the main plane direction of the point by six stress components at any point. The common methods are the algebraic method, the Mohr circle method, and the three-dimensional stress state [26–28].

In this paper, the equilibrium equations and real symmetric matrices in three directions are listed through the three-dimensional stress state, and the eigenvalues are solved. The eigenvalue solution is the main stress, and the first, second, and third principal stresses are distinguished according to the absolute value [29].

$$l\sigma_x + m\tau_{xy} + n\tau_{xz} = l\sigma_n$$

$$m\sigma_y + n\tau_{zy} + l\tau_{xy} = m\sigma_n$$

$$n\sigma_z + l\tau_{xz} + m\tau_{yz} = n\sigma_n$$

The listed real symmetric matrices:

$$A = \begin{bmatrix} \sigma_x & \tau_{xy} & \tau_{xz} \\ \sigma_y & \tau_{zy} & \tau_{xz} \\ \sigma_z & \tau_{xz} & \tau_{yz} \end{bmatrix},$$

Thus, the corresponding triple principal stress: the corresponding triple main direction: the process of solving is the process of A solving eigenvalues [30].

The stress value comparison diagram of different schemes obtained by the processed data is as follows: the comparison diagrams of the stress values of different schemes obtained from the processed data are shown in Figures 12 and 13.

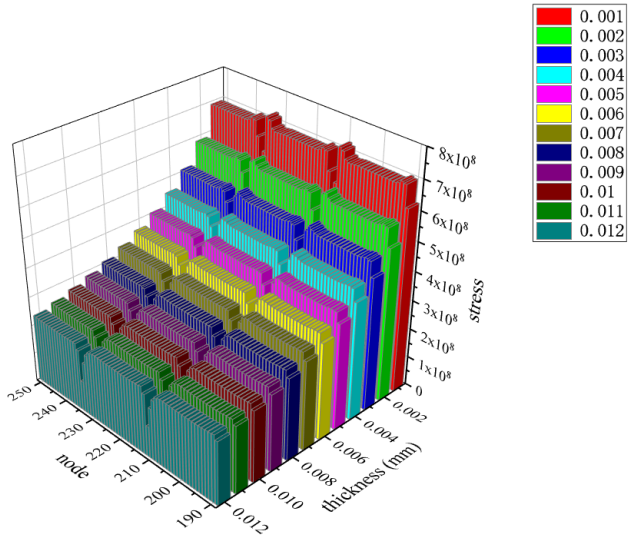


Figure 12. Stress changes under different thicknesses at ply angles of 45, −45, 0.

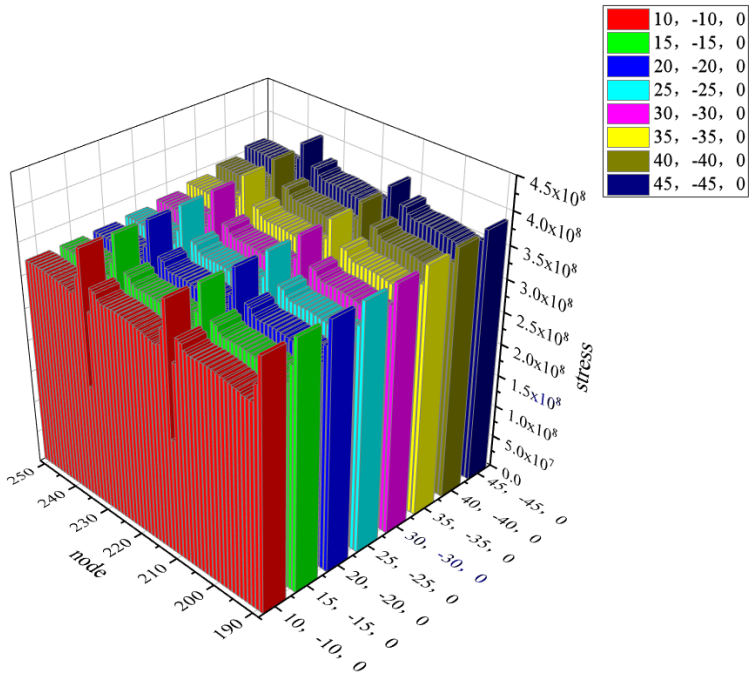


Figure 13. The stress changes of different ply angles under the thickness of 0.002 m.

When the ply angle is 45, −45, 0, the stress value decreases with the increase of the ply thickness, and the decreasing trend become smaller and smaller.

In the case of a thickness of 0.002 m, with the continuous change of the ply angle, the stress value decreases first and then increases, but the change range is not large.

It can be seen from the above that there is no problem with the output stress port and output stiffness matrix port when OpenSees calculates the finite element model, and the output file content is chaotic and will not be arranged in a regular format. Therefore, it is necessary to modify the source program and write the applicable Python or MATLAB program to solve these problems.

2.3. Program Optimization

Combined with the designed ply scheme, if APDL is used for calculation and analysis, only the data results of one scheme can be obtained at a time. For different scheme designs, it is necessary to repeatedly model and modify the parameters, and the output data file also needs to be saved as many times as possible, otherwise, it cannot be retained for subsequent verification. That is, it uses the OpenSees parametric language to calculate, and also needs to write multiple running files and undergo multiple runs to obtain the required data files. Based on these problems, a set of programs that can automatically analyze and process data is written. When writing the TCL file, for the same model, its node coordinates, unit information, constraint settings, load values, etc. are unchanged. What needs to be changed is only the material setting part and some parameters of the file output part. Therefore, only the material parameters of a specific row need to be modified, then multiple TCL files are output cyclically, and then the bat file (input OpenSees running environment variables, as well as the path of various library files) is written. It eliminates the process of compiling in the vs environment, and finally modifies the last line in the bat file so that multiple cmd windows can be opened simultaneously for parallel computing, greatly saving computing time and improving efficiency.

The node displacement diagram and stress cloud diagram under different ply angles obtained after program optimization are shown in Figures 14 and 15:

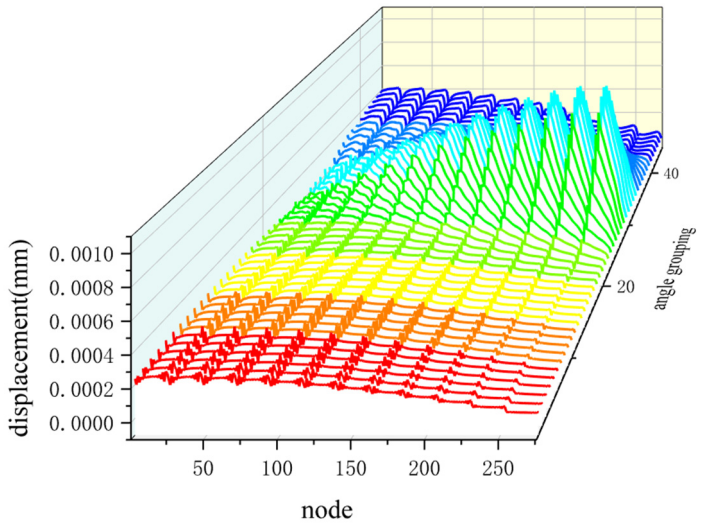


Figure 14. Plus node displacement at different angles output after program optimization.

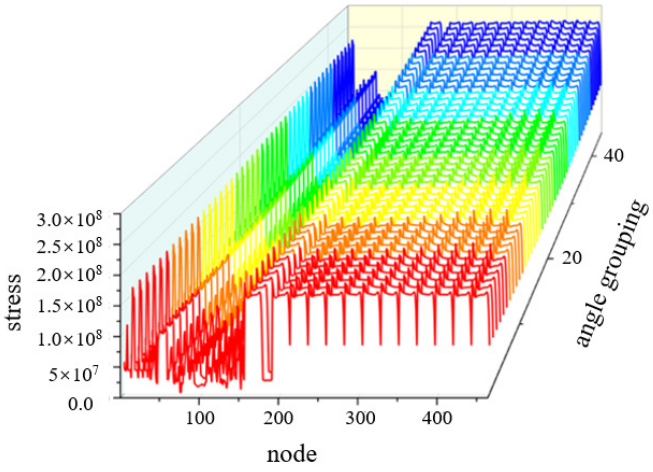


Figure 15. Comparison of stress at different angles after program optimization.

3. Semianalytical Optimization Design

By searching and optimizing a set of independent variable parameters, the objective function reaches the minimum value (maximum value). Since the solution is required to be nonlinear and the derivative function is unknown, the selected solution method is Nelder-Mead. It is an optimization algorithm based on heuristic rules, similar to the common genetic algorithm (generic algorithm, GA) and particle swarm optimization (particle swarm optimization, PSO), through a series of artificially designed rules, starting from the initial value, to iteratively find the optimal solution.

Firstly, a function is defined. The function content is to input three random parameters first, write these parameters into the running file of OpenSees, call OpenSees through Python to calculate the output result file, traverse the data, and return the maximum value. Then, with the help of the Nelder-Mead optimization function, the optimal point is found in the given parameter region, and, finally, the three-parameter values of the optimal point are output. The program logic diagram is shown in Figure 16.

In this paper, after 50 iterations, the data files of thickness, angle value and stress value are returned. After comparative analysis, under the condition of satisfying the maximum allowable stress, the scheme with the smallest stress value is selected. The angle value and thickness value of this optimal scheme are 9.96875 and 0.03325 m respectively. Table 6 lists the results of 20 iterations after function optimization.

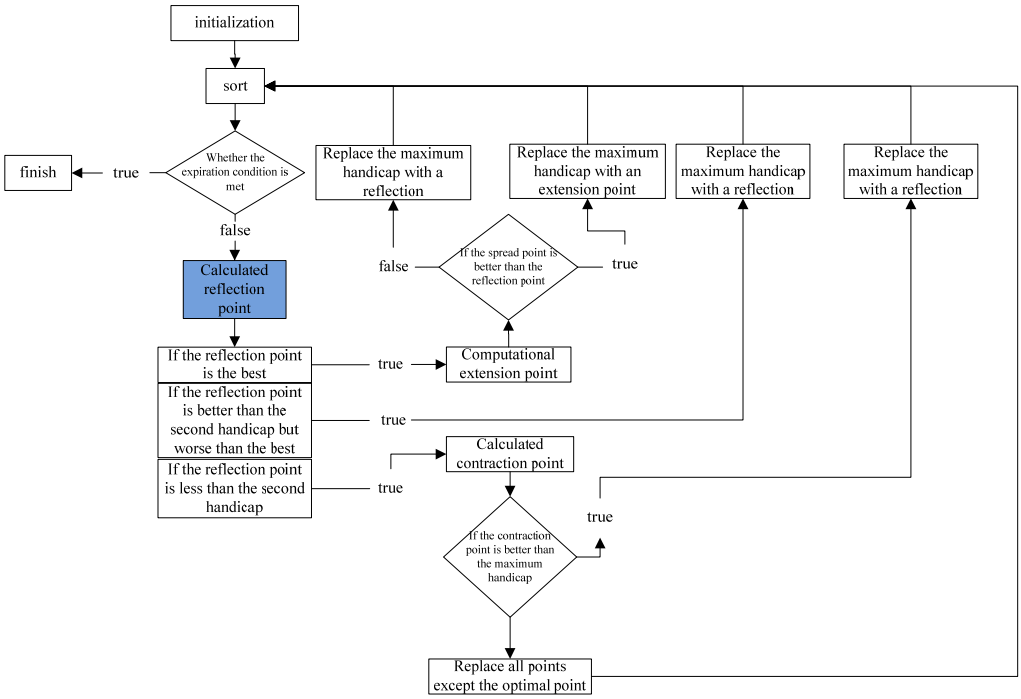


Figure 16. Nelder-Mead function optimization logic diagram.

Table 6. The results of 20 iterations after function optimization.

Thickness/m	Angle	Maximum Stress/Pa
0.002	10°, −10°, 0°	771177281.3985813
0.502	10°, −10°, 0°	771189203.9732419
0.002	10.5°, −10.5°, 0°	772091536.2209214
0.502	9.5°, −9.5°, 0°	772081537.1205486
0.127	10.25°, −10.25°, 0°	771990438.4686378
0.252	10°, −10°, 0°	771991576.4586244
0.002	10.25°, −10.25°, 0°	779181732.3365489
0.252	9.75°, −9.75°, 0°	772124486.4568624
0.0645	10°, −10°, 0°	772094568.7863486
0.017625	10.03125°, −10.03125°, 0°	772013878.7203546
0.03325	10°, −10°, 0°	771838747.0454676
0.002	10.03125°, −10.03125°, 0°	771963483.2436784
0.03325	9.96875°, −9.96875°, 0°	771071532.3645576
0.0098125	10.015625°, −10.015625°, 0°	771346760.1384348
0.017625	10°, −10°, 0°	771546634.1331687
0.002	10.015625°, −10.015625°, 0°	772046877.1363486
0.017625	9.984375°, −9.984375°, 0°	772076781.6875494
0.00590625	10.0078125°, −10.0078125°, 0°	772083644.3133846
0.0098125	10°, −10°, 0°	772097533.6564441
0.002	10.0078125°, −10.0078125°, 0°	771738342.1387745

4. Research Convergence

In order to explore the influence of the number of grids on the finite element analysis of composite pressure vessels, the composite pressure vessel model is meshed. The number of elements 933, 1292, 2086, 4661 is set respectively, and the constraints and loads are set. Then the stress data of the nodes near the maximum stress value are output and compared. The results show that the stress values approach the same, and the output data are shown in Figure 17. The average relative error of 2086 and 4661 elements is 4.35%. Therefore, even if the number of grids increases, the stress value of the same part is less affected, and the stress value tends to converge.

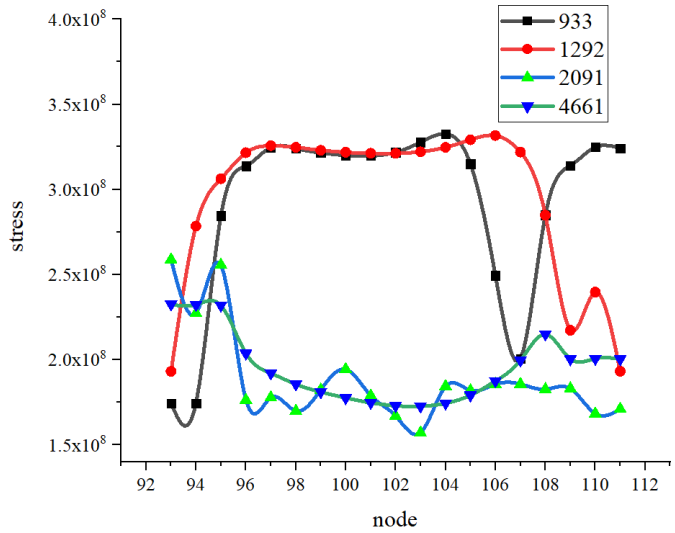


Figure 17. Stress data output of different grid numbers.

5. Conclusions

Through OpenSees, the data obtained from the calculation of composite pressure vessels with different stacking schemes can be seen to show that the thicker the thickness is, the smaller the stress is under the condition of a certain angle. However, the node displacement fluctuates more and more when the thickness increases. Therefore, there is a most suitable thickness to make the stress small and the node displacement changes smoothly. The appropriate thickness is 0.004 mm; in the case of a certain thickness, the larger the ply angle, the more obvious the change of node displacement and the greater the stress. Therefore, there is a most suitable angle to make the stress small and the node displacement change smoothly. The appropriate angle is 25°, −25°, 0°.

When compiling the OpenSees running file and calculating, the OpenSees program architecture is modified, the stress output port and the stiffness matrix output port are improved, and the required stress data are selected through the screening process. The parametric language is used to calculate and analyze, which simplifies the process of modeling and analysis.

The above content is a simplification of the calculation process. With the help of the Python tool, the running file of OpenSees is rewritten to output data files of all different situations. This optimization improves the repeated mechanical labor caused by modifying parameters such as material parameters or fiber ply angle thickness during each calculation. However, this does not find the optimal parameter solution. It is necessary to process the data file and draw the curve to summarize the law. The idea of semianalytical optimization is to optimize a set of independent variable parameters by searching so that the objective function reaches the minimum value (maximum value). Since the solution is required to be nonlinear and the derivative function is unknown, the selected solution method is Nelder-Mead. It is an optimization algorithm based on heuristic rules, similar to the common genetic algorithm (generic algorithm, GA) and particle swarm optimization (particle swarm optimization, PSO), through a series of artificially designed rules, starting from the initial value, to iteratively find the optimal solution. Firstly, a function is defined. The content of the function is to input three random parameters, write these parameters into the running file of OpenSees, call OpenSees through Python to calculate the output result file, traverse the data, and return the maximum value. Then, with the help of the Nelder-Mead optimization function, the optimal point is found in the given parameter region, and, finally, the three-parameter values of the optimal point are output.

This method can deal with the ply structure design of different models well and has important guiding significance for the optimization design of the actual composite structure.

Author Contributions: Software, formal analysis, writing-original draft, B.D.; methodology, writing-original draft, M.Z.; conceptualization, methodology, software, J.Z.; conceptualization, methodology, software, Y.L.; conceptualization, methodology, software, W.J. All authors have read and agreed to the published version of the manuscript.

Funding: This research was funded by the National Key R&D Program of China (Project No. 2020YFB1506104). The authors gratefully acknowledge the support.

Institutional Review Board Statement: Not applicable.

Informed Consent Statement: Not applicable.

Data Availability Statement: All data are included in the paper can be openly obtained.

Conflicts of Interest: The authors declare no conflict of interest.

References

1. Hua, D.; Junpeng, G.; Jianwen, B. Preparation and Mechanical Properties of Aligned Discontinuous Carbon Fiber Composites. *Hangkong Cailiao Xuebao J. Aeronaut. Mater.* **2018**, *38*, 69–74.
2. Littlefield, A.G.; Hyland, E.J. 120 mm Prestressed Carbon Fiber/Thermoplastic Overwrapped Gun Tubes. *J. Press. Vessel. Technol.* **2012**, *134*, 041008. [CrossRef]
3. Azeem, M.; Ya, H.H.; Alam, M.A.; Kumar, M.; Stabla, P.; Smolnicki, M.; Gemi, L.; Khan, R.; Ahmed, T.; Ma, Q.; et al. Application of Filament Winding Technology in Composite Pressure Vessels and Challenges: A Review. *J. Energy Storage* **2022**, *49*, 103468. [CrossRef]
4. Rajak, D.K.; Pagar, D.D.; Kumar, R.; Pruncu, C.I. Recent progress of reinforcement materials: A comprehensive overview of composite materials. *J. Mater. Res. Technol.* **2019**, *8*, 6354–6374. [CrossRef]
5. Yang, H.; Jiazhong, X.U.; Liu, M.; Tianya, J. Design of filament winding pattern for composite dry-fiber reinforced rotary structures. *Acta Mater. Compos. Sin.* **2018**, *35*, 3500–3507.
6. Arhant, M.; Briancon, C.; Burtin, C.; Davies, P. Carbon/polyamide 6 thermoplastic composite cylinders for deep sea applications. *Compos. Struct.* **2019**, *212*, 535–546. [CrossRef]
7. Li, C.; Xie, H.; Liu, L. Research on bearing characteristics of fiber wound ultra-high pressure vessel. *Ordnance Mater. Sci. Eng.* **2019**, *42*, 6.
8. Cohen, D. Influence of filament winding parameters on composite vessel quality and strength. *Compos. Part A Appl. Sci. Manuf.* **1997**, *28*, 1035–1047. [CrossRef]
9. Hirst, M.; Yeo, M.F. The analysis of composite beams using standard finite element programs. *Comput. Struct.* **1980**, *11*, 233–237. [CrossRef]
10. Kennedy, J. Parameter selection in particle swarm optimization. In Proceedings of the International Conference on Evolutionary Programming, San Diego, CA, USA, 25–27 March 1998.
11. Coello, C.; Pulido, G.T.; Lechuga, M.S. Handling multiple objectives with particle swarm optimization. *IEEE Trans. Evol. Comput.* **2004**, *8*, 256–279. [CrossRef]
12. Parsopoulos, K.E.; Vrahatis, M.N. Recent approaches to global optimization problems through Particle Swarm Optimization. *Nat. Comput.* **2002**, *1*, 235–306. [CrossRef]
13. Bergh, F.; Engelbrecht, A.P. A study of particle swarm optimization particle trajectories. *Inf. Sci.* **2006**, *176*, 937–971.
14. Alam, S.; Yandek, G.R.; Lee, R.C.; Mabry, J.M. Design and development of a filament wound composite overwrapped pressure vessel. *Compos. Part C Open Access* **2020**, *2*, 100045. [CrossRef]
15. Cao, Y.; Li, Q.; Yu, L. Analysis and Calculation of the Electromagnetic Field in Permanent Magnet Synchronous Motor Based on ANSYS. In Proceedings of the International Conference on Information Science & Engineering, Zhuhai, China, 26–28 June 2022; IEEE: Piscataway, NJ, USA, 2009; pp. 133–136.
16. Langer, P.; Jelich, C.; Guist, C.; Peplow, A.; Marburg, S. Simplification of Complex Structural Dynamic Models: A Case Study Related to a Cantilever Beam and a Large Mass Attachment. *Appl. Sci.* **2021**, *11*, 5428. [CrossRef]
17. Pervan, N.; Mešic, E.; Colic, M. Stress Analysis of External Fixator Based on Stainless Steel and Composite Material. *Int. J. Mech.Eng. Technol.* **2017**, *8*, 189–199.
18. Chen, D. *Structural Design and Development of Carbon Fiber Wound Type IV Composite Pressure Vessel*; Wuhan University of Technology: Wuhan, China, 2019.
19. Zeng, W. *Research on Winding Process of Glass Fiber Composite Pressure Vessel*; Shanghai Second Polytechnic University: Shanghai, China, 2021.
20. Abdellah, M.Y.; Swailem, S.; Abdel-Jaber, G.; Gomaa, A.A. Finite Element Analysis for Impact Behavior of glass fiber composite laminate. *Int. J. Adv. Sci. Technol.* **2020**, *29*, 3.
21. Wang, Z.; Duan, C.; Luo, X. Strength Analysis and Influence Factors Research of Carbon-Fiber Wound Composite Gas Cylinder with Aluminum Liner. In Proceedings of the ASME Pressure Vessels and Piping Conference, Online, 3 August 2020.
22. Jian, J.; Usmani, A. Modeling of steel frame structures in fire using OpenSees. *Comput. Struct.* **2013**, *118*, 90–99. [CrossRef]

23. Lu, X.; Xie, L.; Guan, H.; Lu, X. A shear wall element for nonlinear seismic analysis of super-tall buildings using OpenSees. *Finite Elem. Anal. Des.* **2015**, *98*, 14–25. [CrossRef]
24. Toscano, R.G.; Dvorkin, E.N. A new shell element for elasto-plastic finite strain analyzes. Application to the collapse and post-collapse analysis of marine pipelines. In Proceedings of the 6th International Conference on Computation of Shell & Spatial Structures, Spanning Nano to Mega, Ithaca, NY, USA, 28–31 May 2008.
25. Mckenna, F. OpenSees: A Framework for Earthquake Engineering Simulation. *Comput. Sci. Eng.* **2011**, *13*, 58–66. [CrossRef]
26. Krysiak, P.; Blachut, A.; Kaleta, J. Theoretical and Experimental Analysis of Inter-Layer Stresses in Filament-Wound Cylindrical Composite Structures. *Materials* **2021**, *14*, 7037. [CrossRef]
27. Sinclair, G.B.; Helms, J.E. A review of simple formulae for elastic hoop stresses in cylindrical and spherical pressure vessels: What can be used when. *Int. J. Press. Vessel. Pip.* **2015**, *128*, 1–7. [CrossRef]
28. Geng, P.; Xing, J.; Wang, Q. Analytical model for stress and deformation of multiple-winding-angle filament-wound composite pipes/vessels under multiple combined loads. *Appl. Math. Model.* **2021**, *94*, 576–596. [CrossRef]
29. Xiao, L.; Wei, X.; Qiang, S. Comparative study on two kinds of push-out tests of PBL shear connectors. *China Civ. Eng. J.* **2013**, *46*, 70–80.
30. Toth, A.; Hasan, I.; Bourauel, C.; Mundt, T.; Biffar, R.; Heinemann, F. The Influence of Implant Body and Thread Design of Mini Dental Implants on the Loading of Surrounding Bone: A Finite Element Analysis. *Biomed. Tech.* **2017**, *62*, 393–405. [CrossRef] [PubMed]

Disclaimer/Publisher's Note: The statements, opinions and data contained in all publications are solely those of the individual author(s) and contributor(s) and not of MDPI and/or the editor(s). MDPI and/or the editor(s) disclaim responsibility for any injury to people or property resulting from any ideas, methods, instructions or products referred to in the content.